

CLINICAL SCIENCE

High resolution magnetic resonance imaging of retinoblastoma

A O Schueler, N Hosten, N E Bechrakis, A J Lemke, P Foerster, R Felix, M H Foerster, N Bornfeld

Br J Ophthalmol 2003;87:330-335

Background/aims: Diagnosis of retinoblastoma is mainly based on indirect ophthalmoscopy, but additional imaging techniques are indispensable for the staging of the disease. A new high resolution magnetic resonance imaging (MRI) technique for the examination of the eye was evaluated. A new surface coil with a diameter of 5 cm allows a field of view of 60 mm with an in-plane resolution of 0.8 mm. We compared preoperative MRI scans with the histology after enucleation in 21 cases of retinoblastoma. Parameters studied were appearance of retinoblastoma, choroidal and scleral infiltration, extraocular extension, optic nerve infiltration, and vitreous seeding.

Results: All retinoblastomas could be visualised as hypointense to vitreous on T2 weighted images and slightly hyperintense to vitreous on plain T1 weighted images with a moderate enhancement after contrast application. Histology revealed seven cases with infiltration of the optic disc or optic nerve. Preoperative MRI scans depict juxtapapillary tumour masses, but it was impossible to differentiate between a juxtapapillary retinoblastoma, a prelaminar infiltration of the optic disc, or a just postlaminar optic nerve infiltration. In five of 14 cases with a proved tumour infiltration of the choroid, MRI scans showed an inhomogeneous contrast enhancement of the choroid in enhanced T1 weighted sequences beneath the retinoblastoma. Whether this sign is specific for a choroidal infiltration or is just an artefact remains unclear. High resolution MRI scans did not allow the exclusion of this form of intraocular tumour extension. All nine cases with proved vitreous seeding were not detected by MRI scans. None of these cases showed scleral infiltration or orbital tumour extension. Therefore, it is not possible to judge the rank of this technique in detecting orbital tumour growth.

Conclusion: The new MRI technique is of limited value in visualisation of prelaminar or postlaminar infiltration of the optic nerve. Advanced choroidal infiltration might be visualised by contrast enhanced T1 weighted MRI scans, but the available spatial resolution did not allow the exclusion this critical form of tumour growth by MRI scans. Nevertheless, high resolution MRI with the new surface coil has superior contrast and spatial resolution compared to computed tomograph (CT) or other available imaging techniques. MRI cannot replace CT in detecting tumour calcification but with increasing experience with this new technique it should be possible to renounce CT scans in the majority of cases of retinoblastoma.

See end of article for authors' affiliations

Correspondence to:
Dr A O Schueler,
Department of
Ophthalmology,
Universitätsklinikum Essen,
Hufelandstrasse 55,
45122 Essen, Germany;
andreas.schueler@uni-essen.de

Accepted for publication
4 September 2002

Treatment of retinoblastoma depends on laterality, intraocular tumour location, and degree of tumour extension. A decade ago standard treatment for advanced bilateral cases was external beam radiotherapy (EBR). Long term follow up revealed a sixfold increased risk for the development of non-ocular malignancies after EBR in patients with a germline mutation in the retinoblastoma gene. The risk of secondary cancer was calculated to be 30% until the age of 30 years.¹ Consequently alternative treatment regimens to replace EBR were evaluated. Most new strategies are based on a systemic polychemotherapy in combination with additional local treatment options like local tumour hyperthermia (chemothermotherapy), brachytherapy, cryocoagulation, or photocoagulation.²⁻⁹ Enucleation is recommended in most unilateral and advanced bilateral cases. Diagnosis is mainly made by indirect binocular ophthalmoscopy under general anaesthesia. Not all tumour parameters, in particular extraocular extension, choroidal infiltration, and optic nerve infiltration, are accessible by ophthalmoscopic examination. Imaging techniques for the verification of the diagnosis and tumour extension are indispensable. Owing to the suspected raised radiosensitivity of patients with the hereditary form of the disease computed tomography (CT) scans were progressively replaced by magnetic resonance imaging (MRI) scans to reduce the exposure to radiation.

The purpose of this study was to investigate a new high resolution technique in MR imaging, using a new ocular surface coil. To test the clinical value of the high resolution MRI in retinoblastoma we compared the preoperative MRI scans with the histological results after enucleation of the affected eyes in 21 cases. Parameters examined in this study were the appearance of the retinoblastoma in MRI scans, tumour extension in the eye, vitreous seeding, infiltration of choroid, sclera and optic nerve, and extraocular extension of the tumour.

PATIENTS AND METHODS

Ocular MR imaging was performed under general anaesthesia with a 1.5 T MR imager (Magnetom SP 63, Siemens AG, Erlangen). A circular surface coil with a diameter of 5 cm was used to improve signal to noise ratio. This coil is a receive only antenna, especially constructed for MR imaging of the eye and protected by a fast fuse. This non-magnetic fuse was introduced to prevent defaults of the second order. For imaging, the children were positioned in the middle of the magnetic field with a 45° tilted head. Each examination included T2 weighted and T1 weighted images. For T2 weighted images a fast spin echo sequence was used.¹⁰ This sequence allowed a repetition time (TR) of 3500 ms and an echo time (TE) of 90 ms in an acquisition time of 6.25

Table 1 Choroidal infiltration

| Case | Reese-Ellsworth classification | Choroidal infiltration | | Optic nerve infiltration | | Vitreous seeding | |
|------|--------------------------------|------------------------|-----|--------------------------|-----|------------------|-----|
| | | Histology | MRI | Histology | MRI | Histology | MRI |
| 1 | Vb | + | + | - | + | + | - |
| 2 | Va | ++ | + | ++ | + | - | - |
| 3 | Vb | + | - | - | + | + | - |
| 4 | Va | + | - | - | + | - | - |
| 5 | IVa | - | - | - | + | - | - |
| 6 | Vb | - | - | + | - | + | - |
| 7 | Vb | (+) | ++ | - | - | + | + |
| 8 | IVa | - | - | - | - | - | + |
| 9 | Va | - | - | - | - | - | - |
| 10 | Vb | + | + | (+) | + | - | - |
| 11 | Vb | (+) | - | - | + | + | - |
| 12 | IIa | (+) | ++ | - | + | - | - |
| 13 | IIb | - | - | (+) | + | - | - |
| 14 | IVa | (+) | - | - | + | - | - |
| 15 | IIIa | + | - | + | + | - | - |
| 16 | Vb | + | - | (+) | - | + | - |
| 17 | IIIa | (+) | - | (+) | + | - | - |
| 18 | Vb | + | - | - | - | + | - |
| 19 | Vb | - | - | - | + | + | - |
| 20 | Va | ++ | - | + | + | - | - |
| 21 | Vb | - | - | - | - | + | - |

Choroidal infiltration: -: no infiltration; (+): Bruch's membrane; +: choroidal infiltration; ++: massive choroidal infiltration; optic nerve infiltration: -: no infiltration; (+): optic nerve head reached; +: prelaminar infiltration; ++: postlaminar infiltration; vitreous seeding: -: absent; +: present.

minutes. The field of view was 120 mm, the acquisition matrix 256 × 256 pixel. The number of excitations (NEX) was two. T2 weighted images were acquired in the transverse plane. The second sequence acquired was a T1 weighted spin echo sequence (TR 600 ms, TE 20 ms, 256 × 256 pixel). With a field of view of 60 mm the in-plane resolution was 0.8 mm. Slice thickness was 2 mm for T2 weighted and T1 weighted images. T1 weighted images were repeated after intravenous application of gadopentetate dimeglumine (Magnevist, Schering AG, Berlin, Germany). A standard dose of 0.1 mmol/kg body weight was administered. Contrast enhanced images were acquired in transverse and sagittal planes.

MR images were scored regarding signal intensity of the tumour compared to vitreous, vitreous seeding of the tumour, infiltration of the choroid, sclera, and optic nerve as well as extraocular extension of the tumour. Evaluation of the MR images was performed before enucleation without knowledge of histology.

Twenty one children with unilateral or bilateral retinoblastoma where enucleation was the only therapeutic option were included in the study. The vast majority of enucleated eyes showed an advanced disease and were virtually blind. Two eyes with Reese Ellsworth group II disease were enucleated because of a suspected tumour infiltration of the optic nerve (Table 1). The mean age at the time of examination was 30 (SD 30.7) months (range 4–130 months). The tumours were bilateral in 12 cases and unilateral in nine cases. In four bilateral cases a primary polychemotherapy with a three drug chemotherapy protocol composed of carboplatin, etoposide, cyclophosphamide, and vincristine was performed for tumour reduction as a part of the treatment plan of the fellow eye in a phase 2 study for the effectiveness of chemothermotherapy in retinoblastoma.¹¹ In two cases (cases 2, 11; Table 1) chemothermotherapy was performed using the neuroblastoma protocol NB 90 (two courses (N1) vincristine, cisplatin and VP16 followed by two courses (N2) vincristine, dacarbazine, ifosfamide and adriamycin).¹² In one case (case 19, Table 1) a late onset recurrence of retinoblastoma after external beam irradiation and polychemotherapy (NB 90) was suspected.

Enucleation was performed using a standard technique with implantation of an hydroxyapatite-silicone implant or a neuropatch coated spherical silicone implant.

The enucleated eyes were fixed in 4% neutral buffered formaldehyde. After 24 hours of fixation the eyes were opened in the direction corresponding to the axis of the MR scans. Serial sections were cut with a layer thickness of 4 µm after dehydration in ascending alcohol series, decalcification in Ossa fixona (trichloroacetic acid, zinc chloride, formaldehyde) if necessary and embedded in paraffin. The optic nerve was examined separately with serial sections.

Cuts were stained with haematoxylin and eosin (HE) and periodic acid Schiff reaction (PAS). On histological examination special emphasis was given to the degree of tumour extension in the eye, vitreous seeding, choroidal infiltration, scleral involvement, and degree of optic nerve infiltration.

RESULTS

Acceptance of examination

Owing to the relatively long image time, it is necessary to perform MRI in children under general anaesthesia or at least under sedation. General anaesthesia is strongly recommended for this examination technique, because the fixation of the surface coil on the eye lids and the positioning with a 45° tilted head in the magnetic field is normally not accepted by the young patients under sedation for the whole duration of the examination. Small motion artefacts markedly reduce the quality of the images. General anaesthesia was used in all of our cases and was well tolerated by all children examined.

Appearance of retinoblastoma in MR imaging

In all cases the retinoblastoma could be visualised by MR images. Retinoblastomas were hypointense to vitreous on T2 weighted images (Fig 1C) and slightly hyperintense to vitreous on plain T1 weighted images (Fig 1A). There was a moderate increase in signal intensity on contrast enhanced images (Fig 1A, C). After application of contrast medium, strong enhancement of the uvea was noted, whereas enhancement of retinoblastomas was less than that of the uvea (Fig 1B).

On enhanced T1 weighted images, finely dispersed areas of very low signal intensity became visible inside the tumour (Fig 1B). They were not visible on either T2 weighted or plain T1 weighted images. By signal intensity and by comparison with histology specimens, they possibly correspond to calcification.

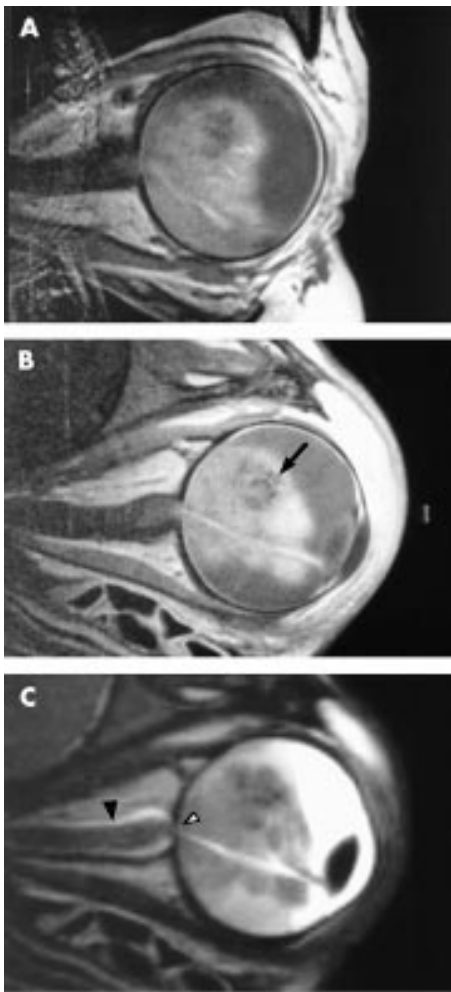


Figure 1 MRI of retinoblastoma (case 3, Table 1). (A) Plain T1 weighted MRI of retinoblastoma. The tumour is slightly hyperintense to vitreous. (B) Contrast enhanced T1 weighted MRI shows moderate enhancement of tumour signal intensity and strong enhancement of the uvea after application of paramagnetic contrast material. Small areas of low signal intensity (arrow) inside the tumour may correspond to calcifications. (C) In T2 weighted images the retinoblastoma is hypointense to vitreous. Hyperintense cerebrospinal fluid inside the subarachnoid space demarcates the optic nerve (black arrowhead). The tumour beside the optic disc (white arrowhead) was interpreted as suspected infiltration.

On plain fast T2 weighted images the cerebrospinal fluid inside the subarachnoid space surrounding the optic nerve, was hyperintense. Inside the cerebrospinal fluid, the low signal optic nerve becomes demarcated and can be evaluated with regard to its diameter (Fig 1C).

Infiltration of optic nerve

Histology revealed a prelaminar optic nerve infiltration in seven cases and a postlaminar optic nerve infiltration in one case. In 14/21 cases MRI scans showed tumour masses next to or overlying the optic disc. In these cases the MRI finding was judged as a possible infiltration of the optic disc (Fig 1C, Table 1). It was impossible to estimate the degree of this infiltration with the available resolution of the scans. In eight of these cases ophthalmoscopy and histology revealed that the retinoblastoma was juxtapapillary without optic disc infiltration. In two cases MRI showed tumour masses at the posterior pole without signs of an infiltration of the optic disc whereas histology revealed a prelaminar infiltration. Postlaminar infiltration of the optic nerve (Fig 2B) in one case was underestimated in MRI scans as probably initial infiltration of the optic

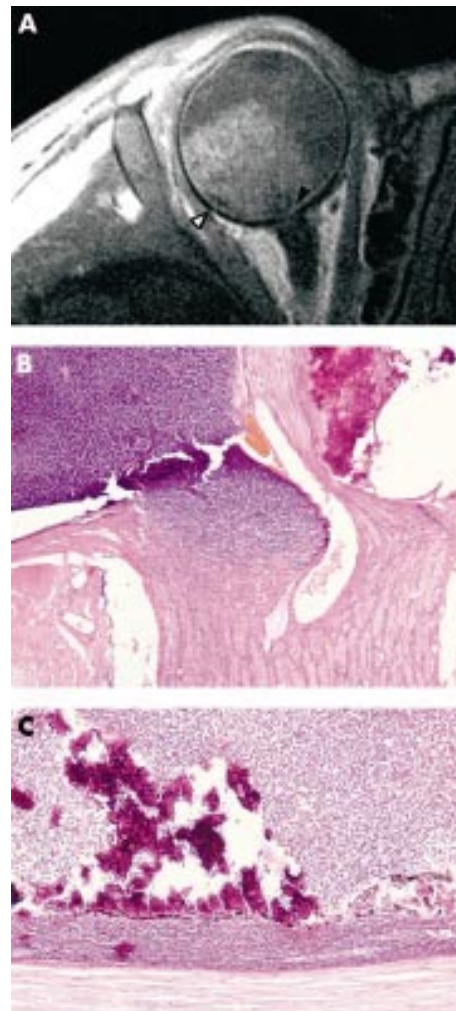


Figure 2 Correlation of MRI and histology (case 2, Table 2). (A) Contrast enhanced T1 weighted MRI showed slight infiltration of the optic disc (black arrowhead) and inhomogeneous contrast enhancement of the uveal band (white arrowhead). Histology revealed postlaminar tumour infiltration of the optic nerve (B) Haematoxylin and eosin staining, $\times 5$ and tumour infiltration of the choroid (C); haematoxylin and eosin staining, $\times 10$.

disc (Fig 2A). In five cases (24%) MRI allowed a correct exclusion of optic nerve infiltration.

In one of the first cases with a dense radiation induced cataract after external beam irradiation and polychemotherapy, MR images showed a cystic extension of the subarachnoid space around the optic nerve in the first 10 mm behind the eye (Fig 4A). The optic nerve inside the cerebrospinal fluid seems to be unchanged. This finding, confirmed in CT scan and ultrasound, was misinterpreted as an extraocular tumour extension and the functional blind eye was enucleated. Histological examination of the optic nerve and the surrounding tissues did not reveal a tumour extension but a thickening of the leptomeninges, that might have been secondary to external beam irradiation (Fig 4B).

Regarding optic nerve infiltration evaluation showed a sensitivity of 75% with a specificity of 38%. The positive predictive value was 43% with a negative predictive value of 71% in our group of patients, with a 38% prevalence of optic nerve infiltration (Table 2).

Choroidal infiltration

Choroidal infiltration of the tumour was found in 14/21 cases on histological examination (prevalence 67%). In two cases, the infiltration involved the whole thickness of the choroid,

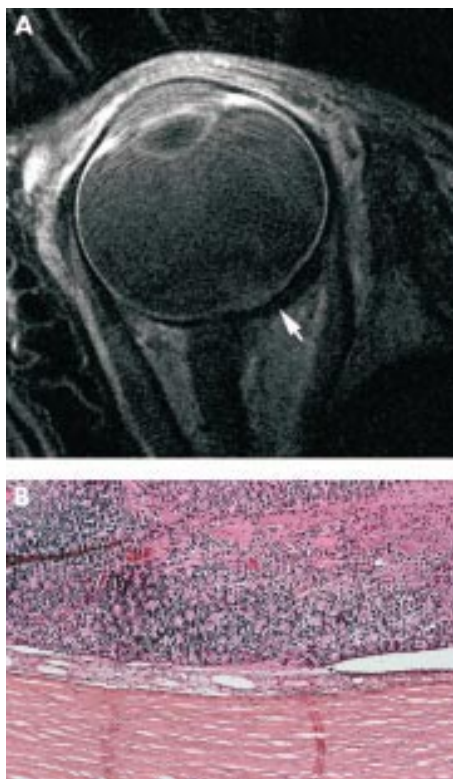


Figure 3 Contrast enhanced T1 weighted MRI of a small retinoblastoma at the posterior pole showed inhomogeneous contrast enhancement (A) of the uvea beneath the tumour (case 12, Table 2). MRI finding can not be explained by histology with infiltration of the uvea beyond Bruch's membrane (B) HE staining, $\times 50$.

whereas in the other 12 cases the infiltration was recognisable just under Bruch's membrane or in a small area of the capillary layer of the uvea (Table 1).

In enhanced T1 weighted sequences normal choroid was recognisable as a homogeneous hyperintense band between sclera and vitreous. MR scans showed, in enhanced T1 weighted sequences in five cases, an inhomogeneous contrast enhancement of the choroid at the base of the retinoblastoma (Figs 2A and 3A). This inhomogeneous enhancement was interpreted as a sign of a possible choroidal infiltration. In all five cases histology confirmed a choroidal infiltration in this area without a correlation between the degree of the infiltration and the appearance in MRI scans (Figs 2C and 3B). In the other nine cases with proved choroidal infiltration MRI was incapable to detect this finding. We got a false positive finding in none of the cases. The sensitivity of MRI in detecting choroidal infiltration was 35% with a specificity of 100%. The positive predictive value was 100% and the negative predictive value was calculated to be 43% (Table 2).

Scleral infiltration and extraocular extension

In plain and enhanced T1 weighted images the sclera was visible as a small hypointense area between choroid and

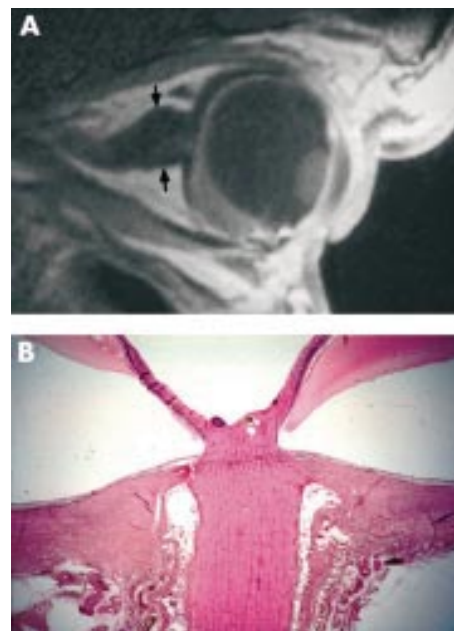


Figure 4 Contrast enhanced T1 weighted MRI (case 17, Table 2). Recurrence of retinoblastoma after external beam irradiation and chemotherapy. Cystic extension of the subarachnoid space around the optic nerve (A) behind the globe was misinterpreted as extraocular tumour extension. Histology (B) showed regressive tumour remnants on the surface of the optic disc. Thickening of the leptomeninges around the optic nerve without extraocular tumour extension. HE staining, $\times 5$.

extraocular tissue (Fig 1A, B). Chemical shift artefacts influence the appearance of the scleral band.¹³ Chemical shift leads to a different spatial registration of the fat and water component of the resulting MR image. This effect was visible in MR images as an apparent broadening of one half of the sclera, whereas the other half seems to be smaller (Fig 1B).

In all of the cases MRI revealed a continuous sclera without signs of scleral infiltration or extraocular extension of the retinoblastoma. Histology confirmed this finding in all cases.

The overall accuracy for excluding extraocular tumour extension by MRI scans was 95% in our series (Table 2).

Vitreous seeding

Vitreous seeding was seen in 8/21 cases by ophthalmoscopy and histological examination (Table 1). In two cases an inhomogeneous density of the vitreous in MR images was interpreted as vitreous seeding of the tumour. In one case with massive vitreous seeding and vitreous bleeding ophthalmoscopy confirmed this finding. In the second case with an inhomogeneous vitreous in MRI scans ophthalmoscopy and histology showed no vitreous seeding.

In the other seven cases with fine dispersed localised or diffuse vitreous seeding of the retinoblastoma it was not possible to detect differences in the density of normal and infiltrated vitreous in plain or in contrast enhanced T2 or T1 weighted images.

Table 2 High resolution MRI in retinoblastoma: diagnostic test results (n=21)

| | Sensitivity | Specificity | Positive predictive value | Negative predictive value | Prevalence |
|--------------------------|-------------|-------------|---------------------------|---------------------------|------------|
| Scleral infiltration | – | 95% | – | 100% | 0% |
| Optic nerve infiltration | 75% | 38% | 43% | 71% | 38% |
| Choroidal infiltration | 35% | 100% | 100% | 43% | 67% |
| Vitreous seeding | 11% | 92% | 50% | 58% | 43% |

– = not calculated.

The sensitivity of MRI in detecting this intraocular form of tumour extension was 11% with a specificity of 92% (Table 1). The positive predictive value was calculated to 50%, the negative predictive value was 58% (prevalence 43%).

DISCUSSION

Exact knowledge of tumour extension is essential for the treatment of retinoblastoma. Imaging techniques are needed to exclude extraocular extension of a retinoblastoma in particular at the posterior pole of the eye. In clinical routine ultrasound is used to determine tumour size and location within the eye. The available resolution of standard ultrasound examination, however, is too low to detect choroidal infiltration or to exclude a limited infiltration of the optic disc or optic nerve.¹⁴ Owing to its low depth of penetration ultrasound biomicroscopy with its increased resolution is only applicable to lesions in the anterior segments of the eye.

Since the late 1970s CT scanning has been the standard imaging technique in the diagnosis of retinoblastoma because of the sensitivity in detecting the typical calcification occurring in about 80% of large retinoblastoma. The presence of calcification in the tumour by CT scan is virtually diagnostic of retinoblastomas.¹⁵⁻¹⁸ However, resolution of CT scans does not allow the non-invasive recognition of an infiltration of the choroid, sclera, or the optic nerve.

MRI was developed as a new imaging technique in the 1980s. In the beginning, MRI had inferior spatial resolution compared to CT, while contrast resolution was always superior. Specialised coils have provided improved spatial resolution available for several organs (knee, spine). At present, MR imaging with its superior contrast resolution is generally recommended as an additional diagnostic method to CT scan in cases of suspected retinoblastoma.¹⁶⁻¹⁹⁻²³ Special coils for the examination of the eye which allow imaging with a field of view as small as 60 mm are just becoming available.²⁴ With these new coils spatial resolution of MRI could be markedly increased. However, a few problems like the presence of motion artefacts, which sometimes occur with long scanning times and low capacity for detecting calcification, are still encountered with this technique.²⁵

We performed MRI scans in 21 cases of retinoblastoma with a newly developed 5 cm surface coil and fast spin echo sequences.¹³ This high resolution MR imaging of the eye is well tolerated without adverse effects in examination of intraocular masses in adults. The new device is suited to detection of very small lesions in the eye with a thickness of less than 1 mm.²⁶ Standard techniques using surface coils with a field of view between 12 and 16 cm and a slice thickness of 3 mm allowed detection of intraocular lesions not smaller than 1.8 mm.²⁷ With an in-plane resolution of 0.8 mm, fast spin echo MR imaging of the eye, with the new specialised surface coil, is a reliable technique to visualise smaller intraocular retinoblastomas. In fast spin echo sequences they appear slightly hypointense compared to vitreous on plane T2 weighted images. In T1 weighted images the retinoblastoma presents as insignificantly hyperintense to the vitreous body. Enhancement with gadopentetate dimeglumine results in a moderate increase of signal intensity in T1 weighted sequences. This appearance of retinoblastoma in MRI with the new surface coil is identical in conventional MRI techniques.²²⁻²⁸⁻²⁹ In some cases small areas of low signal intensity within the intraocular tumour can be observed. These areas of signal dropoff correlate with calcification in the retinoblastoma²¹ but the same sign can be observed in haemorrhage within the tumour. The diagnostic value of this sign is consequently low and not comparable to the diagnostic value of calcification seen in CT scans.

In five cases with proved choroidal invasion scans with the new surface coil showed an atypical heterogeneous contrast enhancement of the choroid at the base of the retinoblastoma.

The reason for this inhomogeneous contrast enhancement of the choroid in these areas with slight choroidal infiltration in enhanced T1 weighted sequences is still unclear and it might be an artefact. If this finding is interpreted as a sign of a tumour infiltration of the choroid, the sensitivity is still low (35%) while specificity and positive predictive value seem to be high (100%). The normal appearance of the choroid in high resolution MRI scans can not exclude the presence of a choroidal infiltration in an individual case.

In this series there was no case with a trans-scleral tumour extension. MRI with the 5 cm surface coil was able to exclude this form of tumour extension in 95% of the cases. As far as a continuous scleral band is detectable in all planes without evidence of extraocular tumour masses, the probability of scleral or orbital infiltration seems to be low; however, very small areas of extraocular tumour spread should not be completely excluded.

Histology of our cases showed prelaminar and slightly postlaminar optic nerve infiltration in eight cases. The available spatial resolution of the new MRI technique still has very limited value in visualisation of prelaminar or slight postlaminar infiltration of the optic nerve.²⁸ In our experience with MRI scans with the new surface coil it is not possible to differentiate between a juxtapapillary tumour and a retinoblastoma with prelaminar infiltration of the optic disc or slight postlaminar optic nerve infiltration. If a massive tumour infiltration of the optic nerve can be visualised by enhanced high resolution MR imaging remains unclear, but the high spatial resolution of this technique might be able to detect this critical form of tumour extension. On plain fast T2 weighted images, the optic nerve becomes demarcated by the cerebrospinal fluid inside the subarachnoid space (Fig 1C). These scans can be examined regarding optic nerve diameter and its contrast enhancement. An enlargement of the retrobulbar subarachnoid space was misinterpreted as extraocular tumour extension (Fig 4A, B). Histology of this case showed a thickening of the leptomeninges that might have been induced by the external beam irradiation years earlier. A moderate enlargement of the subarachnoid space in the retrobulbar region of the optic nerve seems to be a frequent finding in high resolution MRI in children without any histopathological correlation. As a solitary sign it should not be misinterpreted as an extraocular extension of the retinoblastoma. The sensitivity and specificity regarding optic nerve infiltration is disappointing. Nevertheless, MR imaging with the new surface coil shows a higher accuracy than other available imaging techniques.²⁷

In our experience it is not possible to detect or exclude a dispersed vitreous seeding of retinoblastoma by high resolution MRI scans. A dense infiltration of the vitreous by tumour cells, sometimes seen in advanced cases with endophytic tumour growth, might be detectable by MR images even with techniques with a lower spatial resolution.²⁸ In our series one case with a vitreous haemorrhage and a tumour seeding showed an inhomogeneous density of the vitreous in MRI scans. The presence of an additional haemorrhage in this case leads to the presumption that MRI visualised mainly the haemorrhage and not the dispersed tumour cells in the vitreous body.

Authors' affiliations

A O Schueler, N Bornfeld, Department of Ophthalmology, Universitätsklinikum Essen, Hufelandstrasse 55, 45122 Essen, Germany
M H Foerster, N Hosten, Department of Radiology, Klinikum Ernst Moritz Arndt Universität, Friedrich Loeffler Strasse 23, 17487 Greifswald, Germany
N E Bechrakis, Department of Ophthalmology, Klinikum Benjamin Franklin der Freien Universität Berlin, Hindenburgdamm 30, 12200 Berlin, Germany
A J Lemke, P Foerster, R Felix, Department of Radiology, Virchow Klinikum der Humboldt Universität zu Berlin, Augustenburger Platz 1, 13353 Berlin, Germany

REFERENCES

- 1 **Eng C**, Li FP, Abramson DH, *et al*. Mortality from second tumors among long-term survivors of retinoblastoma. *J Natl Cancer Inst* 1993;**85**:1121–8.
- 2 **Shields CL**, Shields JA, De Potter P, *et al*. Plaque radiotherapy in the management of retinoblastoma. Use as a primary and secondary treatment. *Ophthalmology* 1993;**100**:216–24.
- 3 **Shields JA**, Shields CL, De Potter P. Cryotherapy for retinoblastoma. *Int Ophthalmol Clin* 1993;**33**:101–5.
- 4 **Shields JA**, Shields CL, Parsons H, *et al*. The role of photocoagulation in the management of retinoblastoma. *Arch Ophthalmol* 1990;**108**:205–8.
- 5 **Shields CL**, Shields JA, Kiratli H, *et al*. Treatment of retinoblastoma with indirect ophthalmoscope laser photocoagulation. *J Pediatr Ophthalmol Strabismus* 1995;**32**:317–22.
- 6 **Shields CL**, De Potter P, Himelstein BP, *et al*. Chemoreduction in the initial management of intraocular retinoblastoma. *Arch Ophthalmol* 1996;**114**:1330–8.
- 7 **Murphree AL**, Villablanca JG, Deegan WF, *et al*. Chemotherapy plus local treatment in the management of intraocular retinoblastoma. *Arch Ophthalmol* 1996;**114**:1348–56.
- 8 **Murphree AL**, Villablanca JG, Deegan Wfr, *et al*. Chemotherapy plus local treatment in the management of intraocular retinoblastoma. *Arch Ophthalmol* 1996;**114**:1348–56.
- 9 **Toma NM**, Hungerford JL, Plowman PN, *et al*. External beam radiotherapy for retinoblastoma:II. Lens sparing technique. *Br J Ophthalmol* 1995;**79**:112–17.
- 10 **Hosten N**, Lemke AJ, Bornfeld N, *et al*. Fast spin-echo MR imaging of the eye. *Eur Radiol* 1996;**6**:900–3.
- 11 **Bornfeld N**, Schuler A, Bechrakis N, *et al*. Preliminary results of primary chemotherapy in retinoblastoma. *Klin Padiatr* 1997;**209**:216–21.
- 12 **Kremens B**, Herrmann F, Schröder-Berg H, *et al*. Myeloablative consolidation versus maintenance therapy to treat stage IV neuroblastoma. A report from the ongoing German neuroblastoma study (NB 90). *Bone Marrow Transplant* 1994;**14** (Suppl 1):S61.
- 13 **Hosten N**, Lemke AJ, Bornfeld N, *et al*. Fast spin-echo MR imaging of the eye. *Eur Radiol* 1996;**6**:900–3.
- 14 **Coleman DJ**. Reliability of ocular tumor diagnosis with ultrasound. *Trans Am Acad Ophthalmol Otolaryngol* 1973;**77**:677–86.
- 15 **Char DH**, Hedges TR, Norman D. Retinoblastoma. CT diagnosis. *Ophthalmology* 1984;**91**:1347–50.
- 16 **Beets-Tan RG**, Hendriks MJ, Ramos LM, *et al*. Retinoblastoma: CT and MRI. *Neuroradiology* 1994;**36**:59–62.
- 17 **Weber AL**, Mafee MF. Evaluation of the globe using computed tomography and magnetic resonance imaging. *Isr J Med Sci* 1992;**28**:145–52.
- 18 **Bullock JD**, Campbell RJ, Waller RR. Calcification in retinoblastoma. *Invest Ophthalmol Vis Sci* 1977;**16**:252–5.
- 19 **Weber AL**, Mafee MF. Evaluation of the globe using computed tomography and magnetic resonance imaging. *Isr J Med Sci* 1992;**28**:145–52.
- 20 **Balmer A**, Munier F, Uffer S. [Diagnostic imaging of intraocular lesions in the child.] *Klin Monatsbl Augenheilkd* 1998;**212**:252–6.
- 21 **Mihara F**, Gupta KL, Joslyn JN, *et al*. Intraocular hemorrhage and mimicking lesions: role of gradient-echo and contrast-enhanced MRI. *Clin Imaging* 1993;**17**:171–5.
- 22 **Ainbinder DJ**, Haik BG, Frei DF, *et al*. Gadolinium enhancement: improved MRI detection of retinoblastoma extension into the optic nerve. *Neuroradiology* 1996;**38**:778–81.
- 23 **Wycliffe ND**, Mafee MF. Magnetic resonance imaging in ocular pathology. *Top Magn Reson Imaging* 1999;**10**:384–400.
- 24 **Sullivan JA**, Harms SE. Characterization of orbital lesions by surface coil MR imaging. *Radiographics* 1987;**7**:9–28.
- 25 **Smith EV**, Gragoudas ES, Kolodny NH, *et al*. Magnetic resonance imaging: an emerging technique for the diagnosis of ocular disorders. *Int Ophthalmol* 1990;**14**:119–24.
- 26 **Hosten N**, Lemke AJ. A special surface coil for high-resolution ocular MRI. *Front Radiat Ther Oncol* 1997;**30**:20–5.
- 27 **De Potter P**, Flanders AE, Shields JA, *et al*. The role of fat-suppression technique and gadopentetate dimeglumine in magnetic resonance imaging evaluation of intraocular tumors and simulating lesions [see comments]. *Arch Ophthalmol* 1994;**112**:340–8.
- 28 **De Potter P**, Shields CL, Shields JA, *et al*. The role of magnetic resonance imaging in children with intraocular tumors and simulating lesions. *Ophthalmology* 1996;**103**:1774–83.
- 29 **Barkhof F**, Smeets M, van der Valk P, *et al*. MR imaging in retinoblastoma. *Eur Radiol* 1997;**7**:726–31.



High resolution magnetic resonance imaging of retinoblastoma

A O Schueler, N Hosten, N E Bechrakis, et al.

Br J Ophthalmol 2003 87: 330-335

doi: 10.1136/bjo.87.3.330

Updated information and services can be found at:

<http://bjo.bmj.com/content/87/3/330.full.html>

References

These include:

This article cites 29 articles, 9 of which can be accessed free at:

<http://bjo.bmj.com/content/87/3/330.full.html#ref-list-1>

Article cited in:

<http://bjo.bmj.com/content/87/3/330.full.html#related-urls>

Email alerting service

Receive free email alerts when new articles cite this article. Sign up in the box at the top right corner of the online article.

Topic Collections

Articles on similar topics can be found in the following collections

[Eye \(globe\)](#) (543 articles)

Notes

To request permissions go to:

<http://group.bmj.com/group/rights-licensing/permissions>

To order reprints go to:

<http://journals.bmj.com/cgi/reprintform>

To subscribe to BMJ go to:

<http://group.bmj.com/subscribe/>